Combined Device- and System-level Simulation of RF MEMS Switches

Gabriele Schrag, Thomas Künzig, Martin Niessner, G. Wachutka

Institute for Physics of Electrotechnology, Munich University of Technology,
Arcisstr. 21, D-80290 Muniche, Germany; schrag@tum.de

ABSTRACT

We present two problem-adapted modeling approaches for RF-MEMS switches which, in principle, are applicable to any capacitive MEMS device and combine device-level with system-level modeling techniques. The first model has been tailored for detailed investigations on device-level (problem-adapted finite element (FE) model), while the second approach is suited for system-level simulation on the basis of macromodels. Both approaches enable the efficient, but yet physics-based simulation of basic device characteristics; this is demonstrated by comparing the simulation results of the RF MEMS switch designs with optical measurements of their static and dynamic operation.

Keywords: Finite element modeling, tailored modeling, system-level modeling, RF MEMS switch

1 INTRODUCTION AND MOTIVATION

Commonly, finite element analysis (FEA) is the method of choice for detailed investigations of MEMS devices. However, in the case of complex device geometries and several coupled energy domains, this method often entails prohibitively long computation times and poor convergence rates. A systematic methodology for building tailored, time-efficient but, at the same time, physics-based and predictive (i.e. scalable) models is therefore a major challenge in the design of microsystems. In this work, two different approaches meeting these demands will be exemplified by applying them to two variants of RF MEMS switches.

2 PROBLEM DESCRIPTION

A schematic view of the switch designs under consideration is shown in Fig. 1. Both variants have been fabricated by [1]; they consist of a gold membrane suspended from four beams, which can be electrostatically pulled down towards a number of contact pads in order to close an RF signal line.

Switch #1 is built with a sliced membrane, while the membrane of switch #2 is perforated, as displayed in Figs. 2 and 3, respectively.

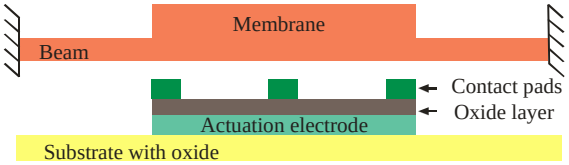

Figure 1. Schematic view of the electrostatically actuated MEMS switches considered in this work.

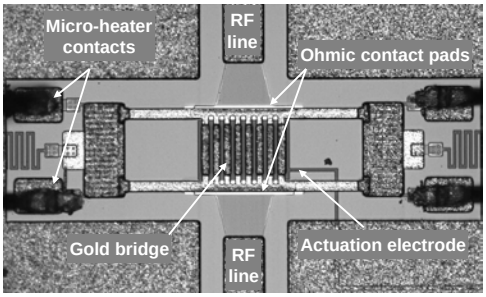

Fig. 2. Microphotograph of switch #1: meander-shaped, resistive heaters are integrated underneath each anchor.

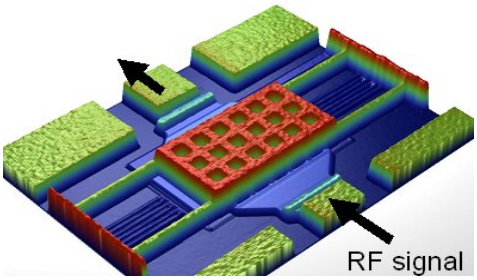

Figure 3. Topographic view of RF MEMS switch #2 as obtained by white-light interferometry.

Physical device models of electrostatically actuated switches have to take into account at least three different energy domains: mechanical domain, electrical domain, and viscous damping by the surrounding air.

Additionally, switch #1 is equipped with a novel thermal recovery capability [2] to counteract stiction caused by microwelding and/or dielectric charging, two phenomena which significantly impair the reliability of such devices. The resistive heaters underneath the anchors enable heating up the bridge, which causes thermo-elastic expansion and exerts shear forces on points prone to sticking. In this way, if failure by stiction occurs, the switch can be reactivated. Thus, for design #1 coupling to the thermal domain has to be taken into account as well.

In order to analyze the efficiency of the restoring mechanism as well as for its optimization, a model is required which delivers sufficiently detailed insight into its internal behavior (e.g., internal heat propagation). It must correctly reproduce all relevant physical effects and their respective couplings, but has still to be fast and efficient enough to be usable for design and optimization studies. In the case considered, the most promising approach is to set-

up a problem-adapted FE-based model as it is described in section 3.1.

The model of switch #2, however, is intended for investigating the switching dynamics. Thus, very fast (i.e., reduced-order) models have to be employed in this case, which yet are physics-based and accurate in order to allow for high-fidelity system simulation. Hence, the appropriate approach is the use of system-level models formulated in terms of generalized Kirchhoffian networks as described in section 4.1.

3 PROBLEM-ADAPTED FE-BASED MODEL OF SWITCH #1

3.1 Modeling

For switch #1, a detailed (3D), coupled, semi-analytical FE-model has been derived including the mechanical, the thermal, and the electrostatic energy domains and the respective couplings between them. In order to make the problem tractable and to keep the computational expense within acceptable limits, Joule heating and electrostatic actuation are described by (semi-)analytical models, and fluidic damping has been taken into account by introducing an empirical damping factor, while the thermo-mechanical interaction is modeled using coupled FEA. Our approach is sketched in Fig. 5 and described in detail in [3].

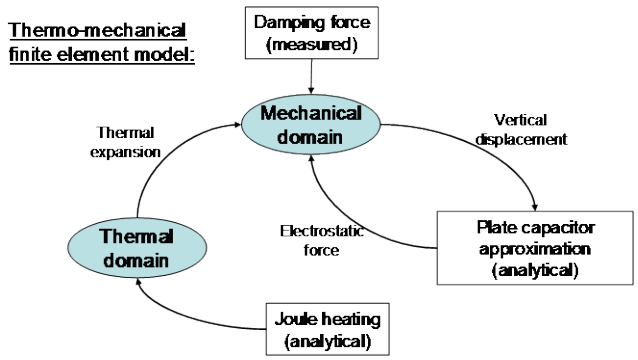

Figure 5. Schematic of problem-adapted FE-based modeling of switch #1. Electrical and fluidic effects as well as Joule heating are included as (semi-)analytical models.

After proper calibration and validation by means of white-light interferomery and Laser Doppler vibrometry, the model allows for evaluating the restoring mechanism in the failure scenario. To this end, a sequential simulation procedure is followed. A solely thermal FE analysis of the device including the substrate (step 1) delivers the temporal evolution of the temperature distribution. Step 2 comprises first a solely mechanical contact simulation (2a) to calculate the deformation of the switch in its closed position. Then the mechanical force on a fixed contact point is extracted (2b). Finally, the transient temperature distribution extracted from step 1 is passed to the thermo-mechanical model as a boundary condition (step 2c) and the total force acting on the welded contact is extracted. Subtracting the mechanical restoring force (obtained by step (2b)) from the finally determined value of the total force then yields the force exerted solely by the thermal recovery mechanism, which constitutes an estimate of its efficiency during failure by stiction.

3.2 Simulation Results

The transient deflection of the bridge depends on the heating time and, hence, is an indirect measure of the heat propagation inside the device. This, in turn, is a decisive parameter for the efficiency of the recovery mechanism, which cannot be directly assessed through measurements. As illustrated in Fig. 6, the transient deflection shows a superimposed oscillation at the mechanical eigenfrequency of the bridge. The very good agreement of simulated and measured data demonstrates the confidence level of the derived model for future investigations.

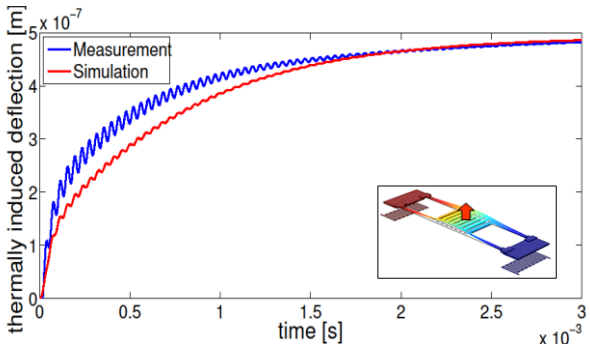

Figure 6: Transient thermal expansion of the gold bridge

Among others, our model reveals the temperature distribution in the interior of the device (see Fig. 7).

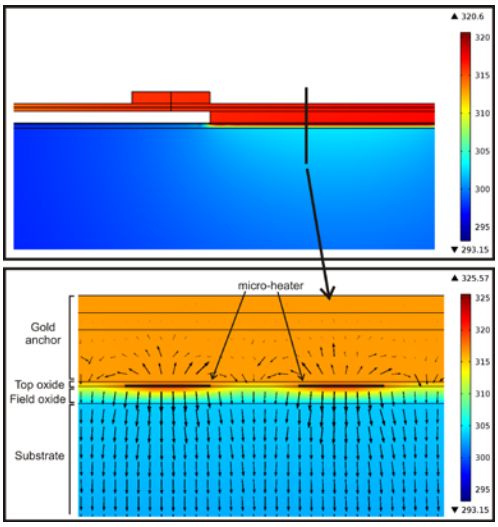

Figure 7. Stationary temperature distribution of two cross-sections of the switch at the hot anchor: the black arrows illustrate the heat flux.

TechConnect Briefs 2016, TechConnect.org, ISBN 978-0-9975-1173-4

It shows that the major temperature rise occurs inside the switch membrane and the hot anchor. However, the largest portion of the heat propagates into the substrate. This underlines the decisive role of the oxide layers between anchor and substrate as a design feature for tuning the heating efficiency. As a consequence, thermally induced forces increase proportionally with increasing thickness of the oxide layer (graph not shown here).

Another important measure for assessing the recovery mechanism is given by the magnitude of the thermally induced force and its variation across the gold membrane. Fig. 8 shows – as expected – no dependence of the mechanical restoring force on position, while the thermally-induced force shows a slight variation along the bridge due to the fact that its value is correlated with the relative volume expansion. However, the maximum variance is only about 25%. The absolute values of the extracted forces, however, range from 180 µN to 220 µN. This turns out to be a promising result, since the exerted forces are of the same order of magnitude as the contact forces reported for welded gold contacts (100 µN -400 µN) in literature [4]. This corroborates the feasibility of the considered design.

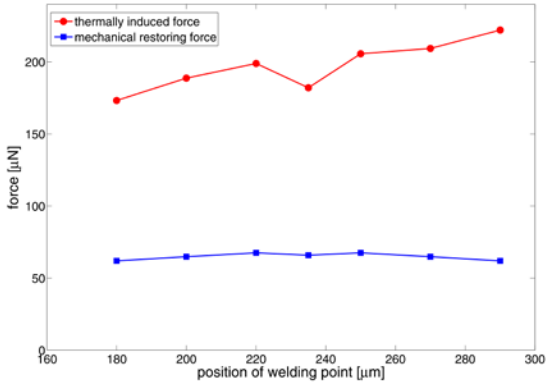

Figure 8. Mechanical and thermally induced forces acting on a point on the membrane prone to stiction as a function of the distance from the hot anchor.

4 SYSTEM-LEVEL MODEL OF SWITCH #2

4.1 Modeling

The model of switch #2 is intended for investigating and optimizing the switching operation of the device, which is governed by mechanical motion including the mechanical contact, by electrostatic actuation, by viscous damping and the respective bidirectional couplings. In contrast to switch #1, an appropriate consideration of the damping forces acting on the switch is crucial, since it essentially determines the switching behavior (e.g., switching time, bouncing of the switch). Hence, it has to be included in the model based on a proper physical description that enables scaling and parameter identification. 3D°transient simulations on finite element level are prohibitive in view of the complex geometry (perforation holes inside the membrane) and the bidirectional fluidmechanical couplings. This is why we pursued a hierarchical modeling strategy leading us to the system-level model of switch #2. The device is decomposed (see Fig. 9) and submodels of each energy domain are built using strictly flux-conserving reduced-order and/or compact modeling techniques within the framework of generalized Kirchhoffian network theory (see°[5]).

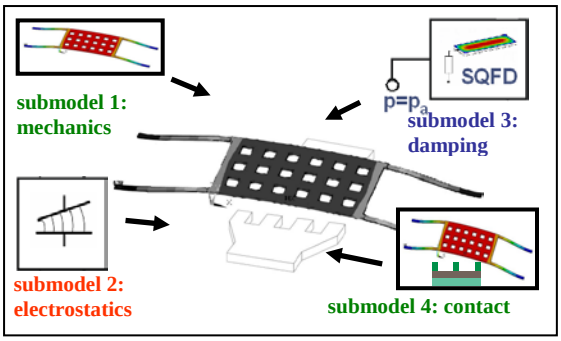

Figure 9. Functional blocks constituting switch #2.

The mechanical submodel of the suspended membrane is derived using the modal superposition technique as described in [6]. Those eigenmodes that are most significant for the switching dynamics are identified and used as basis to formulate a macromodel in terms of the modal amplitudes as state variables, where each of which is governed by a linear second-order differential equation. Residual stress in the suspended membrane is taken into account by calibrating the fundamental eigenfrequency with repect to measurements.

The submodel of the electrostatic domain relies on a differential plate capacitor approach adjusted to the perforated membrane structure. The electrostatic forces are expressed in terms of the modal amplitudes and consistently transferred to the mechanical model.

The viscous damping forces are implemented by applying the mixed-level approach as presented in [7]. It is based on the Reynolds equation, which is evaluated in the gap underneath the moving membrane by a fluidic Kirchhoffian network distributed over the device geometry. At perforations and outer boundaries lumped, physics-based fluidic resistances are added, which describe the additional pressure drops at these locations. Consequently, this mixed-level model does not constitute a pure lumped element model and – depending on the granularity of the finite network – still involves a rather large number of degrees of freedom. However, the advantage of this approach is that it can be tailored to the topography of the real structure, i.e. it is possible to consider all perforations and locally varying gap heights, and it can be generated automatically from a finite element discretization using a purpose-built conversion tool.

The mechanical contact between membrane and contact pads is modelled by introducing contact forces at the respective locations. They are represented as function of the modal amplitudes and contain also higher-order modes

(see°[8]). Therefore, this model allows for emulating the bouncing of the membrane (Fig. 11).

All submodels are connected as part of a generalized Kirchhoffian network, translated into a hardware description language (such as Verilog-A, VHDL-AMS) and linked to form a computationally efficient, physics-based, energy-coupled reduced-order model of the switch, which can be directly implemented in any commercial system-level simulator. The strength of this method is that all submodels are fully parametrized and enable the fast, efficient, and yet physics-based simulation of the transient device behavior, even for complex device geometries.

4.2 Simulation Results

The overall accuracy of the proposed system-level model decisively depends on the accuracy of the constituent submodels and, hence, on their proper calibration and validation. Fig. 10 shows the transient response of the switch to an excitation by a voltage with rectangular waveform. The excellent agreement of simulated and measured data proves that not only the submodels, but also the sophisticated coupling effects are properly implemented (electro-mechanical spring softening in the actuated state as well as increasing viscous damping with decreasing width of the air gap).

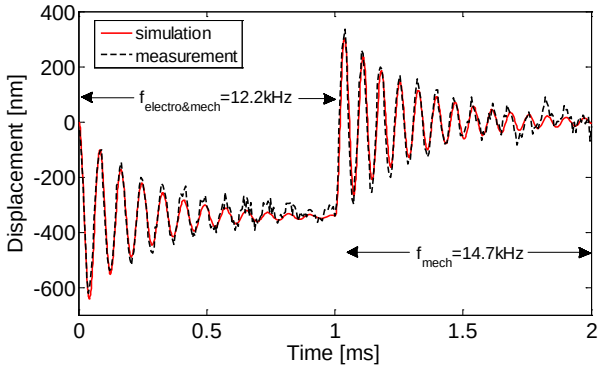

Figure 10. Transient response of the membrane to a rectangular waveform of the driving voltage.

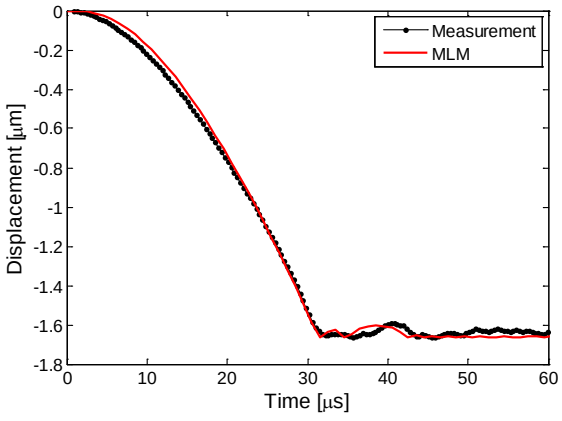

Figure 11. Closing of the switch: comparison between optically measured and simulated displacement.

With the calibrated parameters the model was used to study the switching behavior (see Fig. 11). The comparison with optically measured data shows that the model reproduces the closing of the switch with remarkable accuracy, including the switching time as well as the bouncing after the membrane hits the contact. Hence, the model is currently used to optimize the switch with respect to the switching time, the contact pressure, and the switching voltage and waveform; the latter is tackled by attaching a driver circuit to the fluid-electromechanical system-level model of the switch.

5 CONCLUSIONS

We presented two approaches to derive problem-adapted models for two exemplary RF MEMS switch designs. These models have been derived on the basis of a general, physics-based strategy, which is extendable to any other electro-mechanical-fluidic system. The focus in this work has been laid upon tailoring the respective models to the given specific needs and practicalities with the view to obtaining accurate results on a physical basis with an acceptable computational expense and to have models available for predictive simulations supporting the design and optimization process.

6 REFERENCES

[1] J. Iannacci, F. Giacomozzi, et al., “A General Purpose Reconfigurable MEMS-Based Attenuator for Radio Frequency and Microwave Applications”, in Proc. of EUROCON, 2009, pp. 1201-1209.

[2] J. Iannacci , A. Faes, et al., “An active heat-based restoring mechanism for improving the reliability of RF-MEMS switches”, Journal of Microelectronics Reliability 51-9/11 (2011), pp.1869-1873.

[3] T. Kuenzig, J. Iannacci, G. Schrag, G. Wachutka, “Study of an active thermal recovery mechanism for an electrostatically actuated RF-MEMS switch”, in Proc. of Eurosime 2012, Portugal, 2012.

[4] A. Tazzoli, et al., “ A positive exploitation of ESD events: Micro-welding induction on ohmic MEMS contact.”, Proc. of the Electrical Overstress/ Electrostatic Discharge Symp. 2011, pp 1-8.

[5] G. Schrag, G. Wachutka, “System-Level Modeling of MEMS using Generalized Kirchhoffian Networks – Basic principles”, in “System-level modeling of MEMS”, Wiley, 2013, pp. 19ff.

[6] L. Gabbay, et. al., “Computer-aided generation of reduced order dynamic macromodels”, J. Micro-electrom. Systems, vol. 9, 2000, pp. 262–269.

[7] G. Schrag, G. Wachutka,“Physically based modeling of squeeze film damping by mixed-level system simulation,” Sensors and Actuators A, vol. 97-98; 2002 , pp. 193–200.

[8] M.Niessner, J. Iannacci, G. Schrag, “Mechanical Contact in System-level Models of Electrostatically Actuated RF-MEMS Switches: Experimental Analysis and Modeling”, Proc. of SPIE, 2011, Czech Republic, Vol. 8066, 2011, pp. 80660Y-1-9.